

Design Principles from Glass Sponges for Structurally Robust Lattices

MATHEUS C. FERNANDES¹, JAMES C. WEAVER², JOANNA AIZENBERG^{1,2,3}, AND KATIA BERTOLDI^{1,2,3,*}

¹ John A. Paulson School of Engineering and Applied Sciences – Harvard University, Cambridge, MA 02138

² Wyss Institute – Harvard University, Cambridge, MA 02138

³ Kavli Institute – Harvard University, Cambridge, MA 02138

* Corresponding author: bertoldi@seas.harvard.edu

Compiled October 29, 2018

1 The hexactinellida sponge *Euplectella Aspergillum* species,
2 commonly known as the Venus' Flower Basket, has received
3 significant attention in the engineering and material science com-
4 munities for its remarkable hierarchical design and robustness
5 across many scales. Its fundamental building blocks, called
6 spicules, are constructed using laminated skeletal elements
7 which consist of a central protein-based organic core surrounded
8 by alternating concentric domains of consolidated silica nanopar-
9 ticles (clear glass) and organic interlayers.^[1-3] Remarkably, these
10 spicules are arranged to form a regular and complex square-grid
11 architecture reinforced by a set of double diagonals (a set of
12 two diagonals going in each direction), creating a checkerboard-
13 like pattern of alternating open-closed cells (see fig. 1). Notably,
14 while it has been demonstrated that the laminar architecture
15 of the spicule leads to superior resistance to fracture propa-
16 gation^[4] and the shape of the spicules enhances the overall
17 strength against buckling^[5], the functionality of the complex
18 double diagonal square-grid macroscale structure is still un-
19 known.

20 The macro-scale architecture of the *Euplectella Aspergillum*
21 provides a remarkable example of slender and regular lattice-
22 like material constructed by nature. Such lattice materials have
23 recently demonstrated to offer novel and unique properties,
24 including being light weight,^[6,7] having high energy absorp-
25 tion,^[8] and having the ability to control the propagation of
26 waves^[9] as well as heat flow.^[10-12] Generally speaking, the
27 properties and functionality of such materials are dictated by
28 the node connectivity. In particular, a minimum node connec-
29 tivity of 6 is required for 2D lattice materials to be stretching-
30 dominated, and therefore, more weight-efficient for structural
31 applications.^[13] As such, lattice materials with square archi-
32 tecture (which has a node connectivity of 4) are known to be
33 very unstable when loaded along specific directions (as the only
34 shear resistance arises from the joints)^[14] and typically require
35 diagonal bracings to stabilize them.^[15]

36 In this paper, we use the anatomy of the hexactinellid sponge
37 species *Euplectella Aspergillum* skeletal system as inspiration for
38 the design of mechanically robust lattice materials with square
39 architecture. First, we use a combination of experiments and
40 numerical analyses to understand the overarching mechanical
41 functions driving the particular and regular alignment of trusses
42 found in the sponge. Then, we utilize an optimization algorithm
43 based on the principles introduced by the sponge to determine

44 the configuration of reinforced square lattice that achieve the
45 highest mechanical performance. Therefore, our results indi-
46 cate that the principles used by Nature to design the *Euplectella*
47 *Aspergillum* may guide the design of lattice architectures struc-
48 turally more robust than those currently used in modern devices
49 and infrastructure.

50 To understand the role of the sponge architecture, we start
51 by comparing its performance to that of other three 2D lattices,
52 all based on a square architecture with edges of length L (see
53 Supplementary Materials for details). Specifically, we consider:
54 *Design A* which is inspired by the sponge and comprises a set
55 of double diagonals going in opposite directions (see fig. 2(a));
56 *Design B* which is similar to the sponge design but only contains
57 a single diagonal crossing each of the closed cells (see fig. 2(b));
58 *Design C* which is similar to bracings found in modern structural
59 engineering and contains a crossing set of diagonal beams in
60 every cell (see fig. 2(c)); and *Design D* which has no diagonal
61 reinforcement (see fig. 2(d)). In all our designs we consider
62 struts with rectangular cross section and depth large enough to
63 avoid any out-of-plane deformation. Moreover, to ensure a fair
64 mechanical comparison between the four designs, we keep the
65 total mass constant and for *Designs A, B, and C* we also constrain
66 the ratio between the mass of the diagonals and non-diagonals
67 struts to be identical (see Supplementary Materials for details).

68 We started by testing samples of the four considered designs
69 comprising a tessellation of 6×6 square cells with $L = 1.91$ cm.
70 The samples were fabricated with a multi-material 3D printer
71 \Rightarrow (add model @James) using \Rightarrow name of material \Rightarrow add
72 info here @James and compressed uniaxially using an Instron
73 Model 5969 with 50kN capacity (Figure 2(e)). \Rightarrow switch labels
74 (f) and (e) in Fig 2 The results reported in Figure 2(f) show that all
75 structures are characterized by an initial linear behavior, a sud-
76 den departure from linearity caused by in-plane buckling and
77 catastrophic failure following immediately thereafter. Further-
78 more, it is also important to note that all designs with diagonal
79 reinforcement (i.e. *Designs A-C*) overlay each other in the linear
80 regime. Focusing on the initial linear regime, we find that the dif-
81 ferent diagonal reinforcement designs considered do not impact
82 the structure's overall stiffness (i.e. the initial stiffness of *Designs*
83 A, B and C is identical). *Design D*, as expected, has a higher
84 stiffness because of its thicker vertical and horizontal element's.
85 However, it fails much earlier due to a shorter critical buckling
86 strain. On the other hand, *Design A* (the sponge design) out-

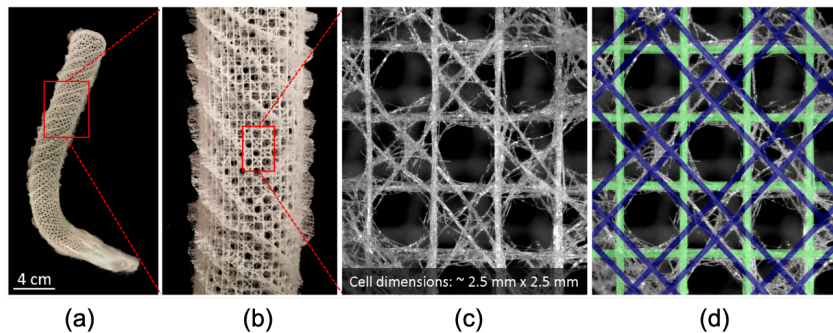


Figure 1: Hexactinellid sponge *Euplectella aspergillum*. (a)-(b) Full-frame photo of sponge. (c) Close up microscope image of the sponge. (d) Comparison between the idealized model (green and blue lines) and the sponge structure.

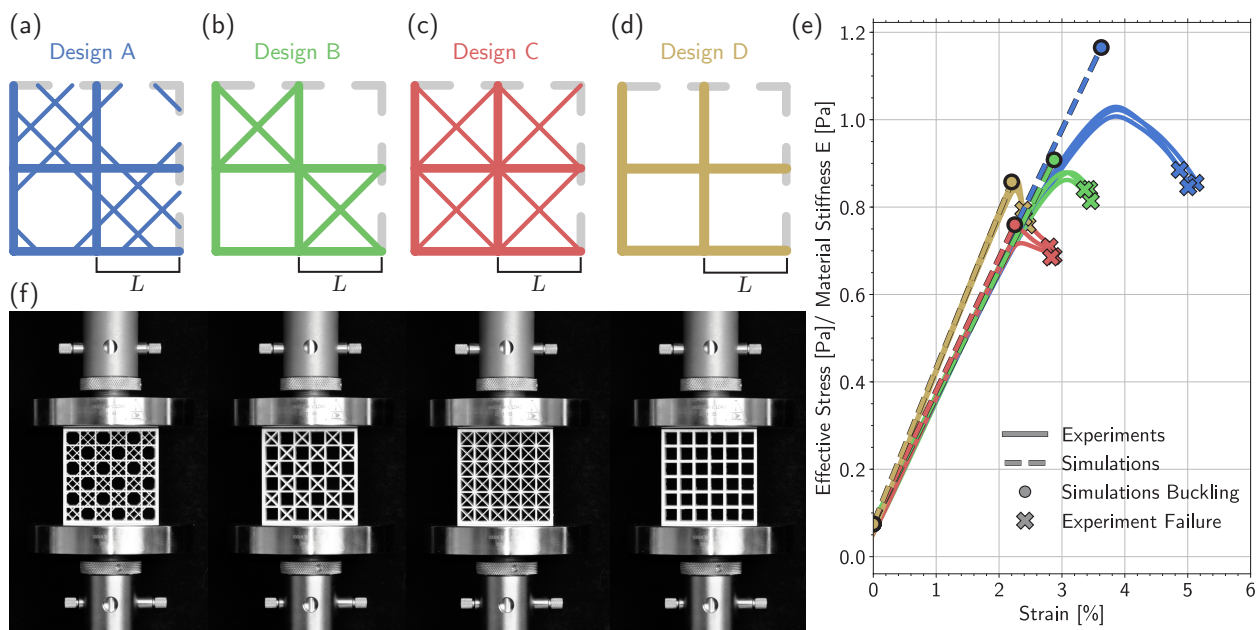


Figure 2: Experimental Results. (a)-(d) shows the different designs (*Design A-D*) considered in this analysis. (e) shows the experimental stress-strain curve as well as the overlaid numerical results for linear stiffness and critical buckling for the different designs considered. (f) shows the undeformed experimental setup for the different designs.

87 performs the considered structures in the amount of load it can
88 bare before the onset of buckling occurs and provides the best
89 mechanical performance without compromising the structural
90 stiffness.

91 Next, we use Finite Element (FE) simulations conducted
92 using the commercial software ABAQUS/Standard to further
93 understand how the double diagonal system found in the *Eu-*
94 *plectella Aspergillum* results in significantly improved mechanical
95 performance. All our models are constructed using Timoshenko
96 beam elements (Abaqus element type \Rightarrow B??) and the ma-
97 terial's response is captured using an isotropic linear elastic
98 materials. We start by simulating the response of the 6 by 6 spec-
99 imens tested in our experiments and find very good agreement
100 between our experiments and numerical model (see Fig. \Rightarrow
101 ??). Having validated our numerical analysis, we next use them
102 to investigate \Rightarrow what??? big picture of Fig 3 the To reduce
103 the computational cost, we took advantage of the periodicity of
104 the structures and investigated their response by considering a
105 Representative Volume Element (RVE) with periodic boundary

106 conditions along the free edges of the unit cell (more informa-
107 tion on this can be found in the SI). For our numerical model
108 we assume Timoshenko beam elements with uniform circular
109 cross-sections and pin-joints at beam intersections. In an effort
110 to create a method for impartial comparison, we maintain a con-
111 stant total mass (or constant volume as the material is assumed
112 to be incompressible) between all of the designs, as well as a con-
113 stant mass ratio between diagonal and non-diagonal elements
114 for designs containing these diagonal reinforcement.

115 The results presented in fig. 3(a) show that all of the struc-
116 tures containing diagonal reinforcement behave the same way
117 for varying loading angles. This illustrates the fact that the struc-
118 tural stiffness is independent of design, but instead depend on
119 the amount of material allocated to the perpendicular aligned
120 beam elements. This is further supported by the graph for *Design*
121 *D*, where all of the material from the diagonal beams is removed
122 and allocated to the non-diagonal elements, giving the structure
123 a higher stiffness at 0° and lower stiffness at 45° . Any stiffness
124 at 45° in *Design D* is strictly a result of the bending resistance

125 due to the pinned joints between the non-diagonal beams.
126 The results shown in fig. 3(b) indicate that the structural buck-
127 ling strength is clearly dependent on the design and alignment
128 of the beam elements. From this figure, we can see that *Design A*,
129 the sponge design, has the highest buckling strength compared
130 to the other designs containing diagonal reinforcement. At 45°
131 loading, Design A improves the buckling strength by a factor
132 of 2.5 times that of *Design C*, which is the commonly used truss
133 systems.

134 **==>write section on Optimization here**

135 In summary, the investigation of the *Euplectella Aspergillum*
136 lum's intricate and regular structure has lead to macro-scale
137 design principles that can be applied to general square lattice
138 materials and structures. When compared with other diag-
139 onally reinforced square lattice designs, the sponge design has
140 experimentally and numerically proven to provide a superior
141 mechanism for withstanding loads prior to onset of buckling.
142 By controlling the number of diagonals, diagonal separation
143 and mass ratio between diagonal and non-diagonal elements, a
144 structure's design can be optimized to withstand buckling load
145 caring capacity.

146 ACKNOWLEDGMENTS

147 This work was partially supported by: NSF-GRFP Fellowship
148 Grant# DGE-1144152 (for M. C. F.), GEM Consortium Fellowship
149 (for M. C. F.), the Harvard Graduate Prize Fellowship (for M.
150 C. F.), **==>add whatever else here**. We would also like to thank
151 James R. Rice, Mark Scott, Joost Vlassak, and Chris Rycroft for
152 insightful discussions.

153

154 REFERENCES

- 155 [1] James C Weaver, Garrett W Milliron, Peter Allen, Ali Mis-
156 erez, Aditya Rawal, Javier Garay, Philipp J Thurner, Jong
157 Seto, Boaz Mayzel, Larry Jon Friesen, et al. Unifying de-
158 sign strategies in demosponge and hexactinellid skeletal
159 systems. *The Journal of Adhesion*, 86(1):72–95, 2010.
- 160 [2] Joanna Aizenberg, James C Weaver, Monica S Thanawala,
161 Vikram C Sundar, Daniel E Morse, and Peter Fratzl.
162 Skeleton of euplectella sp.: structural hierarchy from the
163 nanoscale to the macroscale. *Science*, 309(5732):275–278,
164 2005.
- 165 [3] FE Shulze. Report on the hexactinellida collected by hms"
166 challenger" during the years 1873–1876. *HMS Challenger*
167 *Sci Results Zool*, 21:1–513, 1887.
- 168 [4] Ali Miserez, James C Weaver, Philipp J Thurner, Joanna
169 Aizenberg, Yannicke Dauphin, Peter Fratzl, Daniel E Morse,
170 and Frank W Zok. Effects of laminate architecture on frac-
171 ture resistance of sponge biosilica: lessons from nature.
172 *Advanced Functional Materials*, 18(8):1241–1248, 2008.
- 173 [5] Michael A. Monn, James C. Weaver, Tianyang Zhang,
174 Joanna Aizenberg, and Haneesh Kesari. New functional
175 insights into the internal architecture of the laminated an-
176 chor spicules of euplectella aspergillum. *Proceedings of the*
177 *National Academy of Sciences*, 112(16):4976–4981, 2015. ISSN
178 0027-8424. . URL <http://www.pnas.org/content/112/16/4976>.
- 179 [6] T. A. Schaedler, A. J. Jacobsen, A. Torrents, A. E. Sorensen,
180 J. Lian, J. R. Greer, L. Valdevit, and W. B. Carter. Ultralight
181 metallic microlattices. *Science*, 334(6058):962–965, 2011. .
182 URL <http://science.sciencemag.org/content/334/6058/962>.

- 183 [7] M.F Ashby. The properties of foams and lattices. *Philosophical Transactions of the Royal Society of London A: Mathematical, Physical and Engineering Sciences*, 364(1838):15–30, 2006. ISSN 1364-503X. . URL <http://rsta.royalsocietypublishing.org/content/364/1838/15>.
- 184 [8] A.G. Evans, J.W. Hutchinson, N.A. Fleck, M.F. Ashby, and
185 H.N.G. Wadley. The topological design of multifunctional
186 cellular metals. *Progress in Materials Science*, 46(3):309 – 327,
187 2001. ISSN 0079-6425. . URL <http://www.sciencedirect.com/science/article/pii/S0079642500000165>.
- 188 [9] A Srikantha Phani, J Woodhouse, and NA Fleck. Wave prop-
189 agation in two-dimensional periodic lattices. *The Journal of
190 the Acoustical Society of America*, 119(4):1995–2005, 2006.
- 191 [10] TJ Lu, HA Stone, and MF Ashby. Heat transfer in open-cell
192 metal foams. *Acta materialia*, 46(10):3619–3635, 1998.
- 193 [11] MF Ashby, CJ Seymour, and D Cebon. Metal foams and
194 honeycombs database, 1997.
- 195 [12] Anthony Glyn Evans, JW Hutchinson, and MF Ashby. Multi-
196 functionality of cellular metal systems. *Progress in materials
197 science*, 43(3):171–221, 1998.
- 198 [13] VS Deshpande, MF Ashby, and NA Fleck. Foam topology:
199 bending versus stretching dominated architectures. *Acta
200 Materialia*, 49(6):1035–1040, 2001.
- 201 [14] Lorna J Gibson and Michael F Ashby. *Cellular solids: struc-
202 ture and properties*. Cambridge university press, 1999.
- 203 [15] A Srikantha Phani and Mahmoud I Hussein. *Dynamics of
204 Lattice Materials*. John Wiley & Sons, 2017.

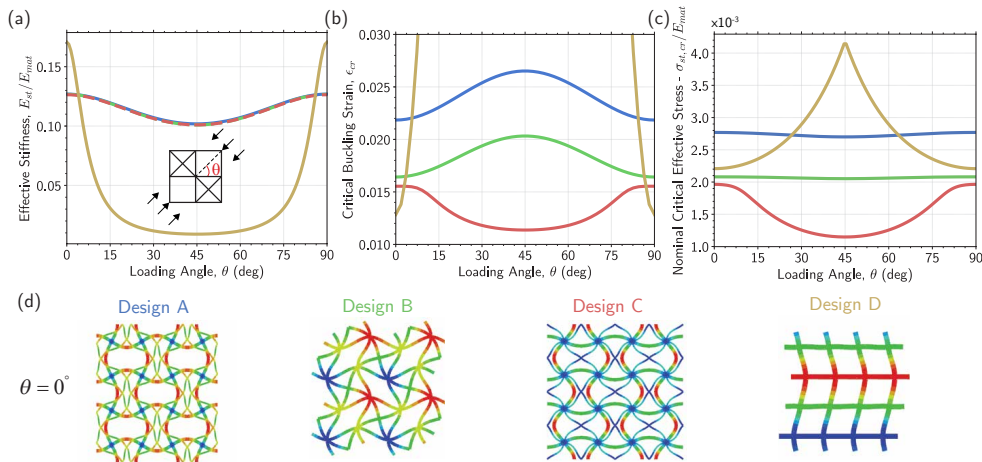


Figure 3: Structure Mechanical Response Figure showing (a) the structural stiffness for the different designs and (b) the buckling resistance for the different designs. The designs considered are depicted below as *Design A-D*.

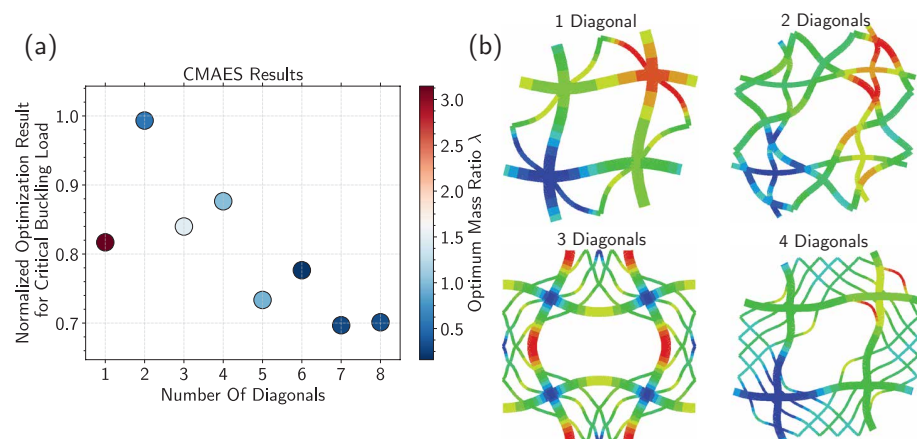


Figure 4: Critical Buckling Load Optimization Results. (a) shows the optimal value of critical buckling load for varying number of diagonals. The color of each point represents the optimal mass ratio λ parameter for that configuration. Note, we do not explicitly show the other optimal values for the diagonal spacing parameters. (b) shows the resulting deformed geometries for designs including one to four diagonals.